THE ASTROPHYSICAL JOURNAL, 535:L87–L90, 2000 June 1

STRUCTURE OF THE CIRCUMNUCLEAR REGION OF SEYFERT 2 GALAXIES REVEALED BY *ROSSI X-RAY TIMING EXPLORER* HARD X-RAY OBSERVATIONS OF NGC 4945

G. MADEJSKI,[1,2] P. ŻYCKI,[3] C. DONE,[4] A. VALINIA,[1,2] P. BLANCO,[5] R. ROTHSCHILD,[5] AND B. TUREK[1,6]

Received 2000 January 19; accepted 2000 April 24; published 2000 May 26

ABSTRACT

NGC 4945 is one of the brightest Seyfert galaxies on the sky at 100 keV, but is completely absorbed below 10 keV; its absorption column is probably the largest that still allows a direct view of the nucleus at hard X-ray energies. Our observations of it with the *Rossi X-Ray Timing Explorer* (*RXTE*) satellite confirm the large absorption, which for a simple phenomenological fit using an absorber with solar abundances implies a column of $(4.5^{+0.4}_{-0.4}) \times 10^{24}$ cm^{-2}. Using a more realistic scenario (requiring Monte Carlo modeling of the scattering), we infer the optical depth to Thomson scattering of ~2.4. If such a scattering medium were to subtend a large solid angle from the nucleus, it should smear out any intrinsic hard X-ray variability on timescales shorter than the light-travel time through it. The rapid (with a timescale of ~1 day) hard X-ray variability of NGC 4945 discovered by us with *RXTE* implies that the bulk of the extreme absorption in this object does *not* originate in a parsec-size, geometrically thick molecular torus. Instead, the optically thick material on parsec scales must be rather geometrically thin, subtending a half-angle less than 10°, and it is likely to be the same disk of material that is responsible for the water maser emission observed in NGC 4945. Local number counts of Seyfert 1 and Seyfert 2 galaxies show a large population of heavily obscured active galactic nuclei (AGNs) which are proposed to make up the cosmic X-ray background (CXRB). However, for this to be the case, the absorption geometry in the context of axially symmetric unification schemes must have the obscuring material subtending a large scale height—contrary to our inferences about NGC 4945—implying that NGC 4945 is *not* a prototype of obscured AGNs postulated to make up the CXRB. The small solid angle of the absorber, together with the black hole mass (of $\sim 1.4 \times 10^6\, M_\odot$) from megamaser measurements, allows a robust determination of the nuclear luminosity, which in turn implies that the source radiates at ~10% of the Eddington limit.

Subject headings: galaxies: individual (NGC 4945) — galaxies: Seyfert — X-rays: galaxies

1. INTRODUCTION

Our current best picture of nuclei of Seyfert galaxies includes the central source (i.e., black hole, accretion disk, and broad-line region) embedded within an optically thick molecular torus (see Antonucci & Miller 1985). The object is classified as a Seyfert 1 for viewing directions which lie within the opening angle of the torus, so that there is a direct view of the nucleus, and as a Seyfert 2 for directions intersecting the obscuring material. The torus absorbs the optical, UV, and soft X-ray nuclear light, so the nucleus in Seyfert 2 galaxies can only be seen at these energies through scattered radiation. A large population of highly obscured active galactic nuclei (AGNs) can make the cosmic X-ray background (CXRB; Madau, Ghisellini, & Fabian 1994; Comastri et al. 1995), so one of central questions toward our understanding of AGNs is whether the torus of the unification models is the same absorbing material as is required for the CXRB models. If so, then the typical torus must be marginally optically thick to electron scattering and subtend a fairly large solid angle to the central source.

NGC 4945 is a nearby (3.7 Mpc; Mauersberger et al. 1996) edge-on starburst galaxy, with intense nuclear IR emission (see Brock et al. 1988) and a "superwind" (Heckman, Armus, & Miley 1990). It also has an active nucleus, first seen unambiguously in *Ginga* X-ray observations (Iwasawa et al. 1993), confirming the Seyfert type 2 classification. These data showed a heavily obscured, strong hard X-ray source above 10 keV, confirmed by the *CGRO*/OSSE observations (Done, Madejski, & Smith 1996), which in turn revealed that NGC 4945 is one of the brightest extragalactic sources in the sky at 100 keV! The absorbing column, a few times 10^{24} cm^{-2}, is among the largest that still allows a direct view of the nucleus at hard X-ray energies since it is optically thick to electron scattering. Thus, it was held to be a prototype of the population of heavily obscured AGNs required to make the CXRB (e.g., Done et al. 1996).

This object is also a megamaser source, detected in the H_2O bands. This implies an edge-on geometry, but the key aspect that makes its study so important is that it is one of only four AGNs for which the black hole mass can be constrained (at $\sim 1.4 \times 10^6\, M_\odot$) from detailed mapping of the megamaser spots (Greenhill, Moran, & Herrnstein 1997). As such, it is one of a few AGNs for which the luminosity in Eddington units can be reliably estimated.

Below we present the data from *RXTE* confirming the large, optically thick absorbing column, but also revealing large-amplitude hard X-ray variability on a timescale of days (we note that the data discussed below have been reported by Madejski et al. 1999, and a similar, large-amplitude variability from NGC 4945 has also recently been observed by *BeppoSAX* [Guainazzi et al. 2000]). Here we show that this implies that the absorber cannot subtend a large solid angle as seen by the nucleus, since electron scattering would smear out the rapid variability on timescales shorter than the light-travel time through such an absorber. Yet this is in conflict with the re-

[1] Laboratory for High Energy Astrophysics, NASA Goddard Space Flight Center, Greenbelt, MD 20771.
[2] Department of Astronomy, University of Maryland, College Park, MD.
[3] Nicolaus Copernicus Astronomical Center, Bartycka 18, 00-716 Warsaw, Poland.
[4] University of Durham, Department of Physics, Durham, DH1 3LE, England, UK.
[5] Center for Astrophysics and Space Sciences, University of California, San Diego, La Jolla, CA.
[6] Department of Physics, Stanford University, Palo Alto, CA.

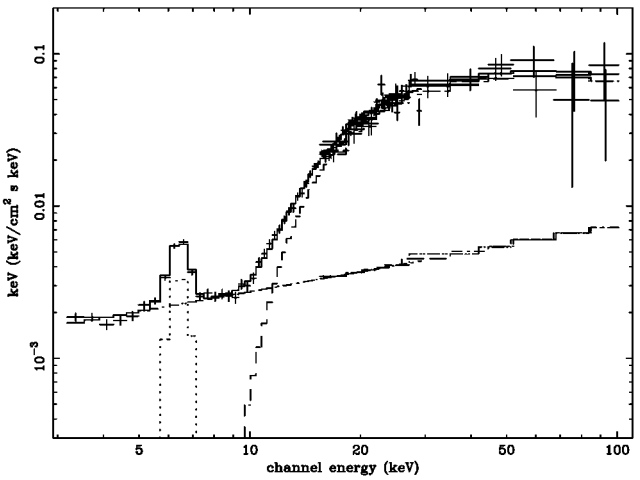

FIG. 1.—Broadband unfolded X-ray spectrum of NGC 4945 as measured with the *RXTE* PCA and HEXTE instruments. The data were fitted with a phenomenological model that includes a hard power-law component photoelectrically absorbed by neutral gas with solar abundances at a column of $4.5 \pm 0.3 \times 10^{24}$ cm^{-2}, with energy spectral index $\alpha = 0.45^{+0.1}_{-0.1}$, exponentially cutting off at 100 keV, plus a nonvariable soft component (assumed to be a power law), and a Fe K line. The observed 8–30 keV flux of the hard component is 5×10^{-11} ergs cm^{-2} s^{-1}.

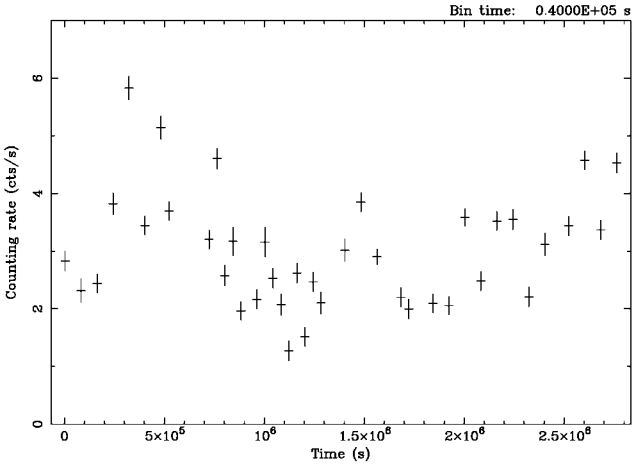

FIG. 2.—Hard X-ray light curve of the Seyfert 2 galaxy NGC 4945 measured with the *RXTE* PCA instrument, showing a rapid, large-amplitude flux variability. Plotted are data from all three layers of three PCA detectors that were turned on during all pointings, over the energy channels nominally corresponding to the range of 8–30 keV.

quirements for the putative torus of the CXRB models, which has to subtend a large solid angle in order to provide a large population of highly obscured AGNs. NGC 4945 is then *not* a prototype for the obscured AGNs that make the CXRB.

2. OBSERVATIONS: SPECTRUM AND VARIABILITY

NGC 4945 was observed by the *Rossi X-ray Timing Explorer* (*RXTE*) satellite for about a month, starting on 1997 October 8. The observations included 38 pointings of ~2000 s each, taken about once per day. The Proportional Counter Array (PCA) and High-Energy X-ray Timing Experiment (HEXTE) data were reduced using standard procedures, resulting in 69,280 s of data from all layers of PCA detectors 0–2 and 18,364 and 19,060 s for HEXTE clusters A and B.

The summed background-subtracted (using the "L7" model) PCA 3–20 keV and HEXTE 20–100 keV data were fitted with a phenomenological model including a hard power law with low-energy photoelectric cutoff (using the cross sections and abundances as given in Morrison & McCammon 1983) and a high-energy exponential cutoff (assumed to be at an energy E_c of 100 keV, in agreement with a compilation of high-energy Seyfert spectra; e.g., Zdziarski et al. 1995 and with the specific results on NGC 4945 from *BeppoSAX* of Guainazzi et al. 2000). Our model also includes a Gaussian Fe K emission line, plus a soft component to model the low-energy spectrum. The resulting fit is shown in Figure 1 and is essentially consistent with the *Ginga*/OSSE results of Done et al. (1996) and *BeppoSAX* data of Guainazzi et al. (2000). The hard power-law (with E_c of 100 keV) energy index α is 0.45 ± 0.1, with absorption of $(4.5 \pm 0.4) \times 10^{24}$ cm^{-2} and an observed 10–50 keV flux of 1×10^{-10} ergs cm^{-2} s^{-1} ($\chi^2 = 80.6/75$ degrees of freedom [dof]). Allowing the cutoff to be unconstrained gave no significant differences, with a best fit of 90^{+130}_{-30} keV.

Here we concentrate on the behavior of the hard, absorbed flux, but for completeness we describe also the lower energy spectrum below ~9 keV. This can be modeled by a power law with energy index 0.57 ± 0.15, with the 1 keV monochromatic flux of 0.001 photons cm^{-2} s^{-1} keV^{-1}, together with an Fe K line at energy of 6.38 ± 0.05 keV, with an intrinsic width σ of 0.37 ± 0.13 keV, a flux of 0.9×10^{-4} photons cm^{-2} s^{-1}, and equivalent width of 1.65 keV, as measured against the continuum detected in the $1^\circ \times 1^\circ$ PCA beam. The soft flux is only 3 times that of the 1 σ fluctuations of the CXRB on the angular scale of the PCA field of view, so we caution that any detailed spectral analysis of the PCA data for this soft component is unreliable. Nonetheless, it is broadly consistent with that seen from *ASCA* and *BeppoSAX*, and a fuller discussion of its origin and extent is given by Brandt, Iwasawa, & Reynolds (1996) and Guainazzi et al. (2000).

The variability of the hard spectral component is plotted in Figure 2. The fluxes of the soft continuum component (below 8 keV), as well as the Fe K line, are consistent with being constant. The hard component (8–30 keV), on the other hand, is highly variable, with a factor of 4 change in 10 days and a factor of 1.7–2 in 1 day between the minimum and maximum flux, and overall rms variance (1 σ) of 0.82 counts s^{-1}. The source was too faint to study the variability with HEXTE.

Could this variability be due to varying absorption? We examined this possibility by modeling separate spectra from high and low count-rate observations. To improve statistics, we coadded the PCA spectra from a number of individual observations with highest and lowest count rates. The two resulting spectra were then fitted using the Monte Carlo absorption model discussed below. We assumed first that the intrinsic source spectrum (and normalization) is the same for both, but the absorption is different—which yielded $\chi^2 = 401/110$ dof—and, second, that the normalization of the intrinsic source flux has changed while the absorption stayed constant, yielding $\chi^2 = 143/110$ dof. This clearly shows that the variability is intrinsic to the unabsorbed nucleus rather than to any change in the absorption column.

With the optical depth to electron scattering of a few, the shape of the absorption cutoff would be different than expected from pure photoelectric absorption, and the detailed shape of the emergent spectrum depends on the geometry (Leahy et al. 1989). We assume an axially symmetric absorber as required in the unification models for Seyfert nuclei and model the spectrum numerically with a Monte Carlo code (Krolik, Madau,

TABLE 1

RESULTS OF MONTE CARLO FITS TO THE *RXTE* DATA FOR NGC 4945 FOR ASSUMED SOLAR AND 2 TIMES SOLAR Fe ABUNDANCES A_{Fe}

	FITTED SPECTRAL INDEX α		FITTED OPTICAL DEPTH τ_e		χ^2 (76 dof)		FRACTION OF DETECTED *UNSCATTERED* PHOTONS	
θ_0[a] (deg)	A_{Fe} = 1	A_{Fe} = 2	A_{Fe} = 1	A_{Fe} = 2	A_{Fe} = 1	A_{Fe} = 2	A_{Fe} = 1 (%)	A_{Fe} = 2 (%)
80	0.7	0.75	2.1	1.5	68.5	68.5	19	31
70	0.7	0.75	2.1	1.5	69.8	68.3	22	35
60	0.7	0.75	2.2	1.5	71.5	72.9	24	39
50	0.8	0.75	2.2	1.6	70.9	69.6	28	42
40	0.7	0.75	2.2	1.6	70.9	72.7	33	48
30	0.8	0.75	2.3	1.6	76.6	74.6	38	55
20	0.8	0.75	2.4	1.6	74.5	77.0	47	63
10	0.8	0.8	2.4	1.7	75.4	79.4	63	76

[a] Assumed half-angle subtended by the torus as seen from the central source.

& Życki 1994), assuming a torus with square cross section where the half-angle subtended by the torus θ_0, its optical depth to electron scattering τ_e, and the power-law index of the incident energy spectrum α are free parameters (the Comptonization cutoff is set to 100 keV as above). The results of our fits (using the PCA data over the range of 3–20 keV and HEXTE data as above) are shown in Table 1, where the 90% confidence regions on α and τ_e are typically ± 0.1.

A small scale height absorber ($\theta_0 \sim 10°$) gives $\tau_e = 2.4$, compared to a large scale height ($\theta_0 \sim 80°$) which gives $\tau_e = 2.1$. With an iron abundance of twice solar, these fits change to $\tau_e = 1.7$ and 1.5, respectively. (Since the photoelectric cutoff present in our data is mainly sensitive to the column density of Fe, larger-than-solar abundance of Fe would make us overestimate the true absorbing column if we assumed solar abundances, and vice versa.) While statistically these might marginally favor the large scale height absorber, we consider that all the fits are probably equally likely given that modeling the spectrum with a fixed cutoff energy may introduce systematic uncertainties. Our calculations include the Fe K emission line produced by the torus, but we also include an additional Fe line (such as may be expected to arise in the photoionized scattering medium). Those calculations also imply that large (>4 times solar) Fe abundances can be excluded: they would imply a stronger Fe K line than is seen in our data.

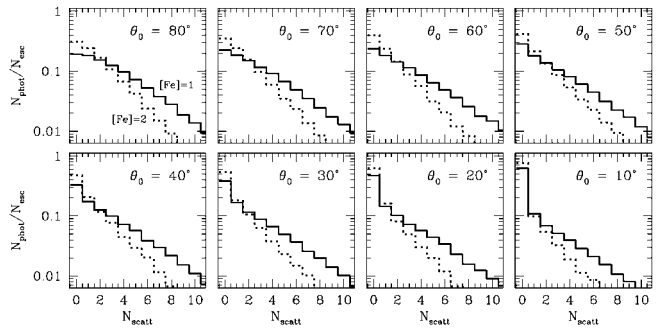

FIG. 3.—Fraction of the observed photons reaching an observer located in the equatorial plane of a torus plotted against the number of scatterings that those photons encountered before reaching an observer. The angle given in each panel is the vertical half-angle θ_0 subtended by the torus as seen from the central source. Iron abundance (relative to solar) is assumed to be 1 (*solid line*) and 2 (*dotted line*), with τ_e equal to the best-fit value for a given Fe abundance and θ_0 (see Table 1). Since the fractional amplitude of variability on short timescales (see Fig. 2) is large (>60%), θ_0 of the optically thick structure must be small, so that the majority of the photons reaching an observer are not scattered.

3. DISCUSSION

The Monte Carlo results described above also give the distribution of the number of scatterings that the photons undergo before reaching the observer positioned in the equatorial plane. This is key in determining the solid angle subtended by the optically thick absorber and thus its vertical size scale. Figure 3 shows the fraction of the observed photons that underwent 0, 1, 2, 3, etc. scatterings before reaching the observer for eight values of θ_0 as discussed above (see Table 1), with the solid and dotted lines showing the results for a solar and twice solar abundance of iron, respectively. The fraction of photons that arrive without being scattered is 19% and 63%, respectively for a "thick" ($\theta_0 = 80°$) and "skinny" ($\theta_0 = 10°$) torus. For 2 times the solar abundance of Fe, these numbers are 32% and 75%. The data in Figure 2 imply that fewer than 40% of the observed photons are scattered over path lengths longer than 1 lt-day, so the half-angle subtended by the optically thick material is less than ~10° for symmetrically distributed absorbing material on size scales greater than several light days from the nucleus. Such a small scale height immediately suggests identification with the water-masing disk material (Greenhill et al. 1997) rather than with the torus of unification models.

If we take the unification models seriously, so that the majority of objects have a torus with similar column density and opening angle, then the ratio of numbers of Seyfert 1 to Seyfert 2 galaxies gives us the geometry of the absorbing material. Current data from hard X-ray surveys indicate that Seyfert 2 galaxies outnumber Seyfert 1 galaxies by a factor of 4 : 1, while the most recent data indicate that at least a quarter and perhaps a half of Seyfert 2 galaxies have columns that are Thomson-thick (see Giommi et al. 1998; Gilli, Risaliti, & Salvati 1999; Maiolino et al. 2000; Risaliti, Maiolino, & Salvati 1999). We can reproduce these numbers with a rectangular cross section torus, classifying the object as a Seyfert 2 if the central flux barely "grazes" the torus, while an object is an optically thick Seyfert 2 only if the line of sight encounters the entire radial distance in the torus. In this context, requiring 1 : 4 : 2 ratios for Seyfert 1 : all Seyfert 2 : optically thick Seyfert 2 galaxies would then imply that the torus has an outer radius of 1.7 times its inner radius r_{in} and equatorial height of $1.7r_{in}$. In this scenario, all Seyfert 2 galaxies are then seen at angles smaller than ~60° from the plane, while the optically thick Seyfert 2 galaxies are confined to angles of ≤45°. Even with only a quarter of Seyfert 2 galaxies being optically thick gives a torus with opening angle of ~50°, while optically thick Seyfert 2 galaxies are confined to angles of ≤12°, i.e., an outer radius of $6.5r_{in}$. Given that the luminosity of the optically thick Seyfert

2 galaxies will be suppressed by electron scattering, then these angles are an *underestimate* of the angular scale height of the torus required to reproduce the relative numbers of Seyfert galaxies.

We repeated the Monte Carlo calculations with the rectangular geometries derived above. Even using the (underestimated) scale height of the torus derived from the smaller fraction of optically thick Seyfert 2 galaxies gives a spectrum in which 50% of the hard X-rays are scattered, still too large to match the observed hard X-ray variability. The large population of obscured objects matches that required for the CXRB, but the geometry of the obscuration derived from applying simple unification schemes to nearby AGNs is plainly inconsistent with that needed in NGC 4945, given the amplitude of its rapid variability.

The variability limits impose constraints on the amount of scattered flux that has lagged on timescales of more than 1 day, but additional information from the shape of the absorption cutoff can also set limits on the size scale in a given geometry. In principle, the variability data alone imply that the absorber could be located close (1 lt-day or less) to the central source, and then it could subtend a large solid angle. However, this would require a high degree of ionization, while the sharpness of the cutoff in the variable hard X-ray spectrum implies that the material is mainly neutral. Spectral fits with the ionized absorption model limit the ionization parameter $\xi = L/(nr^2) \leq 60$, where n is the density of the illuminated material and r is its mean distance from a source of ionizing luminosity L. But we know the absorber has a column of $N_{\rm H} = n\Delta r \sim 10^{24}$ cm^{-2}. In the two geometries derived above, $\Delta r = 0.7r_{\rm in} = 0.8r$ and $\Delta r = 5.5r_{\rm in} = 1.7r$. For an ionizing luminosity $L_{\rm ion}$ of 10^{42} ergs s^{-1} (which is a conservative value, and $L_{\rm ion}$ is likely to be higher, as we argue below), this gives $r \geq L/(\xi N_{\rm H})(\Delta r/r) \sim 10^{16}(\Delta r/r)$ cm, i.e., $r \geq 4$ and $r \geq 6$ lt-days for these two torus geometries. Thus, an axially symmetric absorption geometry that potentially could reproduce the number counts of local Seyfert galaxies (and can be extrapolated to explain the CXRB) cannot be associated with neutral material on size scales of less than several light days from the nucleus: the absorber is most likely distant, and thus geometrically thin, and an obvious candidate for this structure is the masing disk. With this, again, the absorption in NGC 4945 *cannot* be typical of the highly obscured objects that produce the CXRB.

With these arguments for the Thomson-thick absorber subtending a small solid angle in NGC 4945, we can now estimate the true luminosity of the source in terms of its Eddington limit $L_{\rm Edd}$. This is independent of the CXRB question but important in relation to understanding the origin of the hard X-ray emission. The currently popular advection-dominated accretion flow (ADAF) models can produce hard X-ray spectra similar to those observed from both AGNs and the low/hard state of the Galactic black hole candidates, but *only* for luminosities $\leq$(0.02–0.04) $L_{\rm Edd}$: above this limit the ADAF collapses into a standard thin disk (Esin, McClintock, & Narayan 1997). In NGC 4945, our Monte Carlo simulations show that the intrinsic flux must be substantially larger than that observed (by a factor of e^{τ_e}, or times 11 for solar abundances) because any scattered nuclear photons are lost from the line of sight. The 1–500 keV flux, corrected for photoelectric absorption alone, is $\sim 5 \times 10^{-10}$ ergs cm^{-2} s^{-1}, so correcting for the Thomson opacity yields a 1–500 keV intrinsic X-ray luminosity of 10^{43} ergs s^{-1}. Assuming that the thermal (optical/UV/EUV) emission from the accretion disk is roughly equal to the hard X-ray emission gives a total bolometric luminosity of the nucleus of $\sim 2 \times 10^{43}$ ergs s^{-1}. With this and an $M_{\rm BH}$ of $1.4 \times 10^6\ M_\odot$, the source is radiating at $\sim$10% of the Eddington luminosity. This is above the ADAF limit. Even if the abundances are twice solar (where $\tau_e = 1.7$), $L/L_{\rm Edd}$ is at least $\sim$5%. We conclude that the hard X-ray emission from NGC 4945 is unlikely to be powered by an ADAF unless we have significantly overestimated its bolometric luminosity, or underestimated its mass. (We note that similar $L/L_{\rm Edd}$ was also inferred by Greenhill et al. 1997, but the discovery of the rapid hard X-ray variability allows us to determine the source luminosity more accurately, as now we know that relatively few photons are scattered *back* to the line of sight.) NGC 4945 is one of the few AGNs for which this quantity can be calculated robustly, since the mass of the central object is *known*, although not as accurately as in the famous megamaser AGN NGC 4258; the resulting uncertainty in $L/L_{\rm Edd}$ may be a factor of 2, comparable to the effects of the unknown Fe abundance or the ratio of $L_{\rm tot}/L_{\rm X\text{-}ray}$. The resulting $L/L_{\rm Edd}$ is comparable to that inferred for the well-studied Seyfert 2 NGC 1068, although since in NGC 1068 the absorber is completely opaque even to hard X-rays, the central luminosity can be estimated only indirectly. These two AGNs are at the opposite end of the scale to NGC 4258, which radiates at $\sim 10^{-4} L_{\rm Edd}$ or less and thus can well be powered by an ADAF (Lasota et al. 1996).

We thank the *RXTE* satellite team for scheduling the observations allowing the daily sampling, Tess Jaffe for her help with the *RXTE* data reduction via her indispensable script REX, and Julian Krolik for his helpful comments on the manuscript. This project was partially supported by ITP/NSF grant PHY 94-07194, NASA grants and contracts to University of Maryland and USRA, and the Polish KBN grant 2P03D01816.

REFERENCES

Antonucci, R., & Miller, J. 1985, ApJ, 297, 621
Brandt, W. N., Iwasawa, K., & Reynolds, C. S. 1996, MNRAS, 281, L41
Brock, D., Joy, M., Lester, D. F., Harvey, P. M., & Ellis, H. B., Jr. 1988, ApJ, 329, 208
Comastri, A., Setti, G., Zamorani, G., & Hasinger, G. 1995, A&A, 296, 1
Done, C., Madejski, G., & Smith, D. 1996, ApJ, 463, L63
Esin, A., McClintock, J., & Narayan, R. 1997, ApJ, 489, 865
Gilli, R., Risaliti, G., & Salvati, M. 1999, A&A, 347, 424
Giommi, P., Fiore, F., Ricci, D., Molendi, S., Maccarone, M. C., & Comastri, A. 1998, Nucl. Phys. B, 69, 591
Greenhill, L. J., Moran, J. M., & Herrnstein, J. R. 1997, ApJ, 481, L23
Guainazzi, M., Matt, G., Brandt, W. N., Antonelli, L. A., Barr, P., & Bassani, L. 2000, A&A, 356, 463
Heckman, T., Armus, L., & Miley, G. 1990, ApJS, 74, 833
Iwasawa, K., et al. 1993, ApJ, 409, 155
Krolik, J., Madau, P., & Życki, P. 1994, ApJ, 420, L57
Lasota, J.-P., Abramowicz, M., Chen, X., Krolik, J., Narayan, R., & Yi, I. 1996, ApJ, 462, 142
Leahy, D. A., Matsuoka, M., Kawai, N., & Makino, F. 1989, MNRAS, 236, 603
Madau, P., Ghisellini, G., & Fabian, A. C. 1994, MNRAS, 270, L17
Madejski, G. M., Done, C., Życki, P., Rothschild, R. E., Blanco, P., Valinia, A., & Turek, B. 1999, BAAS, 30, 1332
Maiolino, R., et al. 2000, A&A, 355, L47
Mauersberger, R., Henkel, C., Whiteoak, J., Chin, Y.-N., & Tieftrunk, A. 1996, A&A, 309, 705
Morrison, R., & McCammon, D. 1983, ApJ, 270, 119
Risaliti, G., Maiolino, R., & Salvati, M. 1999, ApJ, 522, 157
Zdziarski, A., Johnson, W., Done, C., Smith, D., & McNaron-Brown, K. 1995, ApJ, 438, L63